ESRF	**Experiment title:** Operando SXRD study of the phase transformation in olivine-based cathode materials for Li-ion batteries at superfast (10C-60C) charge regimes	**Experiment number:** MA 4030
Beamline: ID11	**Date of experiment:** from: 06 June 2018 to: 10 June 2018	**Date of report:** 25 September 2018 *Received at ESRF:*
Shifts: 12	**Local contact(s):** Carlotta Giacobbe	

Names and affiliations of applicants (* indicates experimentalists):

Dr. Drozhzhin Oleg*, Lomonosov Moscow State University; Skolkovo Institute of Science and Technology, Moscow, Russia

Dr. Alekseeva Anastasia*, Lomonosov Moscow State University, Moscow, Russia

Tereshchenko Ivan*, Lomonosov Moscow State University; Skolkovo Institute of Science and Technology, Moscow, Russia

Report:

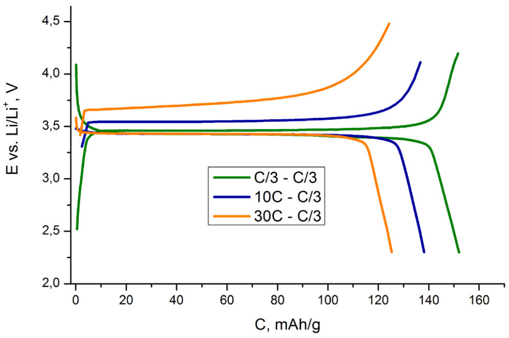

Figure 1. Charge (at C/3, 10C, 30C rates) and discharge (at C/3 rate) curves for $LiFePO_4$.

We studied three olivine-type materials: $LiFePO_4$, $LiFe_{0.5}Mn_{0.5}PO_4$ and $LiFe_{0.25}Mn_{0.75}PO_4$. For analysing phase transformation behavior at different charge rate, we performed the following experiments: a) charge and discharge at C/3 rate (all studied materials), b) charge at 10C and discharge at C/3 rate ($LiFePO_4$, $LiFe_{0.5}Mn_{0.5}PO_4$), c) charge at 30C and discharge at C/3 rate ($LiFePO_4$). X-ray diffraction patterns were collected in *operando* regime. Acquisition time 3 s for each pattern.

Dependence of the capacity and charge-discharge curves on charge rate for $LiFePO_4$ cahode material is presented in Figure 1. Reversible electrochemical specific capacity reaches ≈150, 140 and 130 mAh/g for C/3, 10C and 30C charge rates, correspondingly (C/3 corresponds to full charge for 3 h, 10C – for 6 min, 30C – for 2 min).

Results of the Rietveld refiniment for selected patterns of the abovementioned experiments are presented im Figure 2 and 3. The following conclusions could be made:

a) Two-phase transition behaviour is typical for $LiFePO_4$ at all studied charge rates. Li-rich phase (denoted as LFP) and Li-poor phase (FP) present in the whole range of states of charge (SOC) during Li^+ deintercalation.

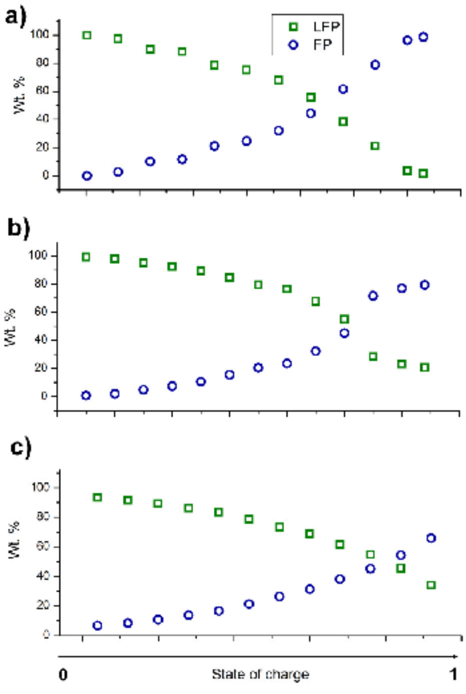

Figure 2. Mass ratio of Li-rich (LFP) and Li-poor (FP) phases during Li^+ deintercalation at C/3 (a), 10C (b) and 30C (c) rates for $LiFePO_4$

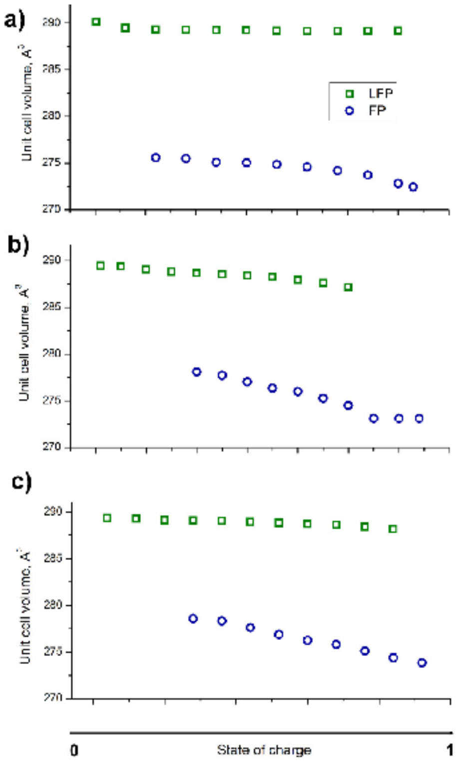

Figure 3. Unit cell volume of Li-rich (LFP) and Li-poor (FP) phases during Li^{+} deintercalation at C/3 (a), 10C (b) and 30C (c) rates for $LiFePO_4$

b) LFP/FP mass ratio changes non-linearly during charge. Non-linearity increases with charge rate.

c) Variation of unit cell parameters of the both LFP and FP phases increases with charge rate. It reduces the volume misfit between Li-rich and Li-poor phases. At C/3 rate, a difference of 4.8% is observed at the beginning of FP phase formation. At 30C the difference is 3.4%. High rate of Li^{+} extraction leads to "smothing" of the phase transformation mechanism. However, we did not observe complete transition to solid solution-type reaction.

In case of $LiFe_{0.5}Mn_{0.5}PO_4$ cathode material, charge at C/3 and 10C rates provides ≈ 140 and 110 mAh/g discharge capacity (Fig. 4). In fact, such behavior eliminates advantage of Mn-substituted olivines (high average potential and therefore enhanced energy densuty) at high charge rates. Hovever, an interesting feature of the $LiFe_{0.5}Mn_{0.5}PO_4$ cathode material is swithing from 3-phase to 2-phase reaction (Fig. 5) at elevated charge rates. As in the case of $LiFePO_4$, high rate of Li deintercalation leads to smoothing of the phase transformations: Li-rich and intermediate phases "split" into one with prolongated region of solid solution $Li_{1-x}Fe_{0.5}Mn_{0.5}PO_4$.

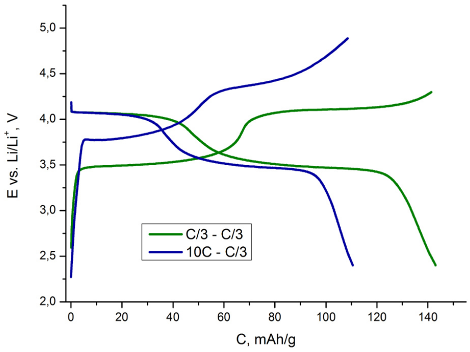

Figure 4. Charge (at C/3, 10C rates) and discharge (at C/3 rate) curves for $LiFe_{0.5}Mn_{0.5}PO_4$.

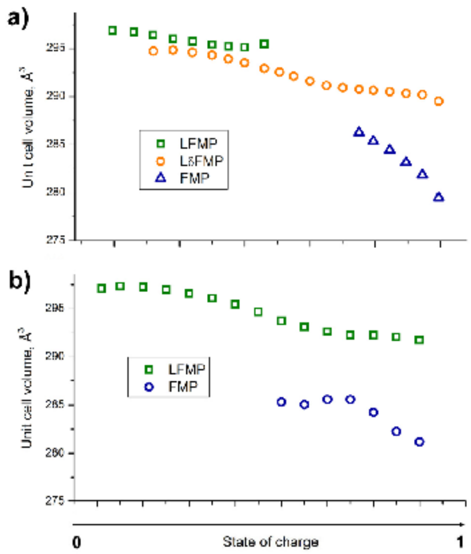

Figure 5. Unit cell volume of Li-rich (LFMP), intermediate (LδFMP) and Li-poor (FMP) phases during Li^{+} deintercalation at C/3 (a) and 10C (b) rates for $LiFe_{0.5}Mn_{0.5}PO_4$.

This feature gives a hope of succesful application of Mn-substituted olivines as high charge rate cathodes after optimisation of the particle size and electrode composite conductivity. However, $LiFe_{0.25}Mn_{0.75}PO_4$ sample exhibits much worse behavior at elevated charge rates: less than 40% of its nominal capacity was retained after charge at 10C current density (Fig. 6). One of the possible reasons of such poor electrochemical properties is large volume change between initial and charged states (Fig. 7): 8.4% for $LiFe_{0.25}Mn_{0.75}PO_4$ vs. 6.4% for $LiFe_{0.5}Mn_{0.5}PO_4$ and 6.1% for $LiFePO_4$.

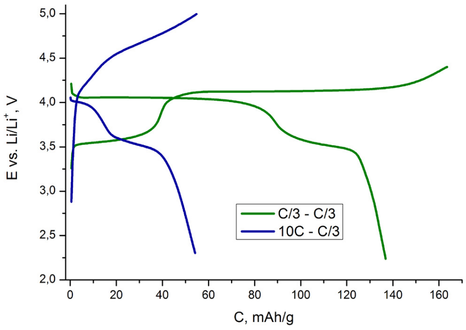

Figure 6. Charge (at C/3, 10C rates) and discharge (at C/3 rate) curves for $LiFe_{0.25}Mn_{0.75}PO_4$.

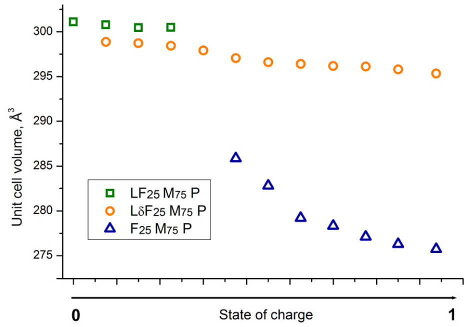

Figure 7. Unit cell volume of Li-rich (LF25M75P), intermediate (LδF25M75P) and Li-poor (F25M75P) phases during Li^{+} deintercalation at C/3 rate for $LiFe_{0.25}Mn_{0.75}PO_4$.

As a brief conclusion, we may assume that increasing charge rate in olivines leads to smoothing of the volume misfit and increase of the solid solution regions of the Li-rich and Li-poor phases. However, complete transition to single-phase behavior was not observed even at 30C current density. $LiFePO_4$ exhibits the best ability of fast charging. Increase in Mn content requires optimisation of the synthetic and electrode fabrication conditions.